Acta Cryst. (1999). B**55**, 841–848

Determination of the modulated structure of $Sr_{14/11}CoO_3$ through a (3 + 1)-dimensional space description and using non-harmonic ADPs

O. Gourdon,[a] V. Petricek,[b] M. Dusek,[b] P. Bezdicka,[c] S. Durovic,[d] D. Gyepesova[d] and M. Evain[a]*

[a]*Laboratoire de Chimie des Solides, IMN, UMR C6502 CNRS – Université de Nantes, 2 rue de la Houssinière, BP 32229, 44322 Nantes Cedex 3, France,* [b]*Institute of Physics, Academy of Sciences of the Czech Republic, Na Slovance 2, 182 21 Praha 8, Czech Republic,* [c]*Institute of Inorganic Chemistry, Academy of Sciences of the Czech Republic, 250 68 Rez u Prahy, Czech Republic, and* [d]*Institute of Inorganic Chemistry, Slovak Academy of Sciences, Dubravska cesta 9, 842 36 Bratislava, Slovak Republic. E-mail: evain@cnrs-imn.fr*

(*Received 18 January 1999; accepted 7 May 1999*)

Abstract

$Sr_{14/11}CoO_3$ (*i.e.* $Sr_{14}Co_{11}O_{33}$, tetradecastrontium undecacobalt tritriacontaoxide), a new phase in the hexagonal perovskite Sr_xCoO_3 system, has been prepared and its structure solved from single-crystal X-ray data within the (3 + 1)-dimensional formalism. $Sr_{14/11}CoO_3$ crystallizes in the trigonal symmetry, $R\bar{3}m(00\gamma)0s$ superspace group with the following lattice parameters: a_s = 9.508 (2), c_s = 2.5343 (7) Å, **q** = 0.63646 (11)**c*** and V_s = 198.40 (13) Å^3. With the commensurate *versus* incommensurate test not being conclusive, the structure was considered as commensurate (*P*32 three-dimensional space group), but refined within the (3 + 1)-dimensional formalism to a residual factor R = 0.0351 for 47 parameters and 1169 independent reflections. Crenel functions were used for the oxygen and cobalt description and a Gram–Charlier expansion up to the third order of the atomic displacement parameter was employed for one Co atom. The structure is similar to that of $Sr_{6/5}CoO_3$, but with a different sequence of the octahedra and trigonal prism polyhedra along the [CoO_3] chains. An interesting feature evidenced by the non-harmonic expansion is the displacement of the prismatic Co atoms from the site center, towards the prism rectangular faces.

1. Introduction

$Sr_6Co_5O_{15}$, a low-temperature form of the brownmillerite-type $Sr_2Co_2O_5$ phase, has been the object of numerous studies. Before being adequately characterized as a stoichiometric hexagonal perovskite phase by Harrison *et al.* (1995), it was considered either as cobalt deficient ($SrCo_{1-u}O_x$; Takeda *et al.*, 1986*a*,*b*) or oxygen deficient ($SrCoO_{3-x}$; Rodriguez *et al.*, 1986; Battle *et al.*, 1988; Bezdicka *et al.*, 1993). The structure determination of such a phase was severely impeded for several years because of a lack of single crystals and also because the structure was assumed to be directly related to the 2H-$BaNiO_3$ type (Bezdicka, 1993). The $Sr_6Co_5O_{15}$ structure can actually be considered as built from isolated infinite columns of face-sharing CoO_6 groups (four octahedra and one trigonal prism), separated by Sr atoms. It can also be described as a stacking of mixed [A_3X_9] and [$A_3A'X_6$] layers, in that sense resembling many other hexagonal phases (Darriet & Subramanian, 1995; Dussarat *et al.*, 1995). However, it is more conveniently described as a modulated composite compound of formulation $Sr_{6/5}CoO_3$ and wavevector **q** = 3/5 **c***. Indeed, with such an approach, initially devised for hexagonal perovskites by Ukei *et al.* (1993) for $[Ba]_x(Pt,Cu)O_3$ and Onoda *et al.* (1993) for $Sr_{1.145}TiS_3$ and recently improved in our work on $Sr_{1.2872}NiO_3$ (Evain *et al.*, 1998), the hexagonal perovskite phases can be simply described within the frame of a unique general model. For instance, all structures are found with the same (3 + 1)-dimensional symmetry and are described

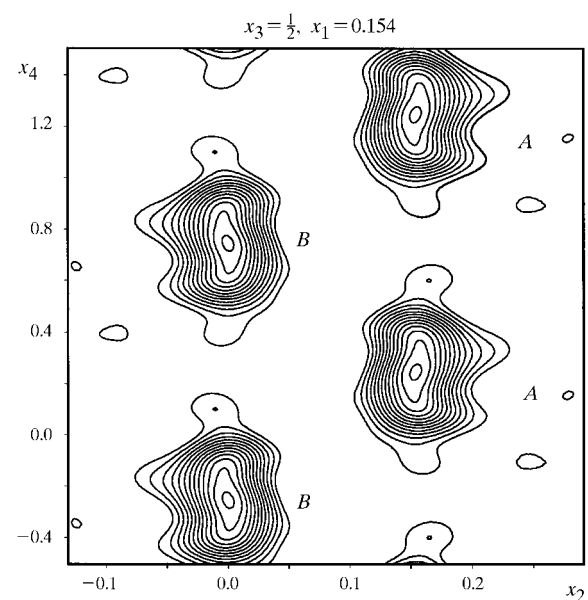

Fig. 1. − x_2x_4 section at x_1 = 0.154 and $x_3 = \frac{1}{2}$ [indicated by a dashed line in (I)]) of the Fourier contour map showing the O atoms [with the O atom on the (m_x 1|0,0,0,$\frac{1}{2}$) mirror plane and using displacive waves only].

with the same (3 + 1)-dimensional superspace group. In addition, a long-period superstructure with low three-dimensional symmetry can be easily refined within that model. This latter advantage enables very good structure determination which otherwise would be very difficult with a conventional three-dimensional approach, as demonstrated by a recent study (van Smaalen, 1995) and in the present work.

In the search for large enough, good $Sr_{6/5}CoO_3$ single crystals, two new phases of composition $Sr_{14/11}CoO_3$ ($Sr_{14}Co_{11}O_{33}$) and $Sr_{24/19}CoO_3$ ($Sr_{24}Co_{19}O_{57}$) were obtained. In this report we present the single-crystal X-ray diffraction structure determination of modulated $Sr_{14/11}CoO_3$. The structure was refined from a twinned crystal data set, within a higher-dimensional space formalism (Janssen *et al.*, 1993) and in combination with a Gram–Charlier non-harmonic development (Trueblood *et al.*, 1996, and references therein) of the atomic displacement factor for one Co atom. The results are compared with those obtained for $Sr_{6/5}CoO_3$ (Harrison *et al.*, 1995) and $Ca_{3/2}CoO_3$ (Fjellvag *et al.*, 1996).

2. Experimental

2.1. *Synthesis and characterization*

Single crystals of $Sr_{14/11}CoO_3$ were grown by heating a mixture of reagent-grade $SrCO_3$, $CoCO_3$ and KOH in the Sr:Co:K molar ratio 1:1:10 for 10 min at 1025 K in an alumina crucible, reheating for 10 min at 1373 K. The mixture was then cooled down to room temperature in the furnace. The final product was recovered from the melt by washing with distilled water. Finally, the crystals were dried at 373 K.

The as-prepared single crystals were firstly examined by electron microprobe. They were found to be free of Al. However, they contained some traces of K (< 1%). The X-ray powder diffractogram revealed diffraction lines similar to those obtained from samples prepared by conventional powder methods (Bezdicka, 1993; Rodriguez *et al.*, 1986).

2.2. *Data collection*

Given the expected low symmetry, the rather long period of the superstructure and the potential twinning (quite common in those materials), a severe screening of potentially good crystals was carried out by means of a Weissenberg camera. Crystals were selected based upon their size and the sharpness of their diffraction spots. A further selection was realised through rapid scans on a Stoe IPDS diffractometer. Both measurements clearly showed the misfit character of the structure (that is, the two subsystems were distinctly visible), but the **q** wavevector could not be accurately derived from the Weissenberg photographs.

Table 1. *Crystallographic data for $Sr_{14/11}CoO_3$*

	(3 + 1)-dimensional commensurate option	
Physical, crystallographic, and analytical data		
Formula	$Sr_{14/11}CoO_3$	
Crystal color	Dark brown	
Molecular weight (g mol^{-1})	2402.91	
Crystal system	Trigonal	
Space group and t section	$R\bar{3}m(00\gamma)0s$, $t = 3/4 \Rightarrow P32$	
Temperature (K)	293	
Cell parameters (from 577 2θ positions obtained from the IPDS measurement)		
a (Å)	9.508 (2)	
c (Å)	2.5343 (7)	
	q = 0.63646 (11), **c*** $\simeq$ 7/11 **c***	
V (Å^3)	198.40 (13)	
Z	3	
Density (g cm^{-3})	5.412	
Crystal description	Needle	
Crystal size (mm^3)	~0.16 × 0.03 × 0.03	
	Enraf–Nonius CAD-4F	Stoe IPDS
Data collection		
Monochromator	Oriented graphite (002)	
Radiation	Mo K-$L_{2,3}$ (λ = 0.71073 Å)	
Scan mode	$\omega/2\theta$	ω
No. of measured reflections	11 872	13 531
hkl range	$0 < h < 14$	$-10 < h < 10$
	$-14 < k < 14$	$-10 < k < 10$
	$-44 < l < 44$	$-30 < l < 31$
sin θ/λ range	0–0.8	0–0.57
No. of standard reflections	3	–
Frequency of standard reflections (s)	3600	–
Data reduction		
Linear absorption coefficient (cm^{-1})	317.3	
Absorption correction	Analytical	
T_{min}/T_{max}	0.14/0.25	0.10/0.23
Scaling selection criterion	$I > 10\,\sigma(I)$	
Scaling coefficient (I_{IPDS}/I_{CAD4})	1.409 (2)	
Number of reflections	25 403	
No. of independent reflections	4551	
Criterions for observed reflections	$I > 3\sigma(I)$	
R_{int}(obs)	3.2	
No. of observed reflections	1169	
Refinement		
Refinement	F	
$F(000)$	298	
No. of reflections used in the refinement	1169	
Twin matrices	$\begin{pmatrix}1&0&0\\0&1&0\\0&0&1\end{pmatrix}, \begin{pmatrix}-1&0&0\\0&-1&0\\0&0&1\end{pmatrix}$	
Twin fractions (%)	11.32 (6), 88.68	
R†	0.0351	
wR†	0.0351	
S	1.06	
No. of refined parameters	47	
Weighting scheme	$w = 1/[\sigma(F_o)^2 + (0.01\lvert F_o\rvert)^2]$	
Difference Fourier residues (e Å^{-3})	[−1.2, +1.7]	

† $R = \Sigma\lvert\lvert F_o\rvert - \lvert F_c\rvert\rvert/\Sigma\lvert F_o\rvert$. $wR = [\Sigma w(\lvert F_o\rvert - \lvert F_c\rvert)^2/\Sigma w\lvert F_o\rvert^2]^{1/2}$.

The best quality crystal was retained and two different data collections were realised. Firstly, the main reflection intensities were collected up to rather high sin θ/λ (0.80 Å^{-1}) on a CAD4-F Nonius diffractometer. Secondly, the satellite (and main) reflection intensities were obtained through long-exposure time measurements on the Stoe Image Plate system, which was configured to medium resolution (IP at 80 mm, limiting sin θ/λ to 0.57 Å^{-1}). Both data sets agreed on a primitive Bravais hexagonal lattice with the following supercell parameters: $a \simeq 9.50$ and $c \simeq 35.4$ Å. From 577 reflection 2θ positions obtained from the IPDS measurement and with a (3 + 1)-dimensional index formalism, the cell parameters and **q** wavevector could be refined with a modified version of the *U-Fit* program (Evain, 1992) to the following values: $a_s = 9.508$ (2), $c_s = 2.5343$ (7) Å, $\mathbf{q} = 0.63646$ (11)$\mathbf{c}^*$ and $V_s = 198.40$ (13) Å^3. The reflection indices for the [CoO_3] first subsystem and the [Sr] second subsystem are obtained from the (3 + 1)-dimensional higher space four indices with the following matrices, respectively,

$$W^1 = \begin{pmatrix} 1 & 0 & 0 & 0 \\ 0 & 1 & 0 & 0 \\ 0 & 0 & 1 & 0 \\ 0 & 0 & 0 & 1 \end{pmatrix}$$

and

$$W^2 = \begin{pmatrix} 1 & 0 & 0 & 0 \\ 0 & 1 & 0 & 0 \\ 0 & 0 & 0 & 1 \\ 0 & 0 & 1 & 0 \end{pmatrix}.$$

Within the e.s.d., the **q** wavevector γ component can be considered as rational and equal to 7/11. Consequently, the $Sr_{14/11}CoO_3$ misfit structure can be either incommensurate or commensurate. In fact, since both models yield similar results (see below), the structure will be discussed, for simplicity, as commensurate. For data collection details, see Table 1.†

2.3. *Data processing*

The data treatment, refinements and Fourier syntheses were all carried out with the *Jana*98 program package (Petricek & Dusek, 1998), using Yamamoto's formalism for the calculation of the structure factors (Yamamoto, 1982). After the usual data reduction intensity decrease correction (< 1%) and absorption correction (Gaussian integration method), the two sets of reflections were adjusted to a common intensity level by applying a scale factor obtained from common reflections with $I/\sigma(I) > 10$. The highly redundant set of 25 403 reflections was then merged according to the $\bar{3}m$ point group [$R_{int}(I) = 0.032$], yielding 4544 independent reflections, of which 1169 with $I/\sigma(I) > 3$ were used for refinements.

2.4. *Refinements*

2.4.1. *(3 + 1)-dimensional incommensurate option*. Considering the $h - k - l = 3n$ general condition and the *hhlm*:$m = 2n$ special reflection condition, the structure refinement was started in the $R\bar{3}m(00\gamma)0s$ trigonal centrosymmetric superspace group. Although possibly commensurate, the structure was initially considered as incommensurate, thus precluding an *a priori t* section choice. The refinement strategy that was adopted is very similar to that used for $Sr_{1.2872}NiO_3$ (Evain *et al.*, 1998). Here are the major characteristics of that strategy.

A first key feature was the positioning of the O atoms of the [CoO_3] first subsystem. An obvious choice would be the occupation of a position on the (m_x1|0,0,0,1/2) mirror plane (Ukei *et al.*, 1993), as depicted in (I).

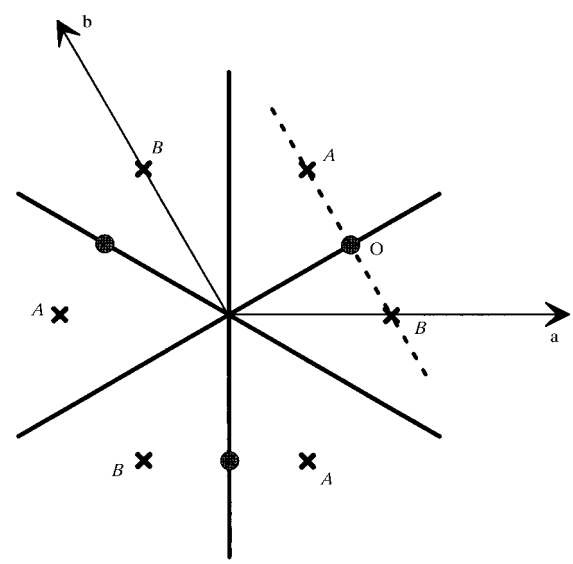

(I)

However, an accurate description of oxygen positions then requires a very large number of displacive waves. In fact, it can be seen in the Fourier synthesis map presented in Fig. 1 that the O atoms never reside on the mirror, but occupy the two self-excluding *A* and *B* positions. Therefore, a better method to describe the O atoms consists of introducing the oxygen on a more general position, with a Crenel function for its occupancy to exclusively generate either the *A* or *B* positions. This is presented in Fig. 2(*a*), with the *A*+ or *A*− (*B*+ or *B*−) referring to the $z = \frac{1}{2}$ and $z = -\frac{1}{2}$ coordinates, respectively. Not only does this choice considerably reduce the number of parameters, but it also leads to much more realistic interatomic distances (the description of a Crenel by means of a Fourier series leading

† Supplementary data for this paper are available from the IUCr electronic archives (Reference: LC0015). Services for accessing these data are described at the back of the journal.

quite often to non-realistic positions). The refinement was thus initiated with the following conditions: an O atom at (0.155, 0.155, $\frac{1}{2}$) with an occupation given by a Crenel function of width $\Delta^O = \frac{1}{2}$ and centered at $\hat{x}_4^O = \frac{1}{4}$, a Co atom at (0,0,0) and, within the second subsystem, a strontium atom at ($\frac{1}{3}$,0,$\frac{1}{4}$). The latter z coordinate, *i.e.* $z(\mathrm{Sr}) = \frac{1}{4}$, is not arbitrary, it is determined by the relative position of the two subsystems along the z axis. An orthogonalization procedure was introduced for the oxygen to reduce the correlations (Petricek *et al.*, 1995). With such a model and using anisotropic displacement parameters, the refinement smoothly converged to a residual factor of $R \simeq 0.21$ upon successive addition of displacive waves for Co [up to the fourth order for the position and to the fourth for the Debye–Waller factor (DWF)], O (second order for position and first order for DWF) and Sr (fourth order for position and second order for DWF). The introduction of the obverse/reverse twin law, very common in those trigonal systems, improved notably the results with a residual factor dropping to $R \simeq 0.16$ for 35 parameters. At this stage of the refinements, the analyses of the Fourier difference maps indicated large residues around the Co position, although several position and DWF waves had been used for its description.

The second major step of the refinement strategy involves solving the problem of the cobalt position. In Fig. 2(*a*), one notices that the Crenel function introduces, as a function of t, two possible combinations for successive O atoms along the [CoO_3] chain: an A/B association, which corresponds to an octahedron coordination for Co, and an A/A (or B/B) association, which leads to a trigonal prism coordination for Co. With totally different coordinations, the Co atoms are expected to behave differently (in position and DWF). Therefore, a new Crenel function was introduced for Co to differentiate the cobalt in octahedra (Co1) from those in trigonal prisms (Co2), as indicated in Fig. 2(*b*). With the splitting of the initial Co position, and reducing the

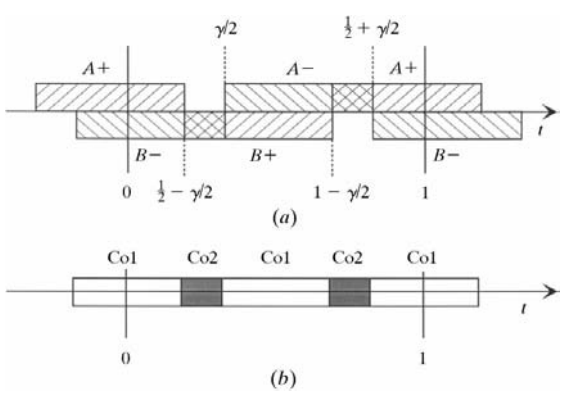

Fig. 2. Domain limits of the various Crenels used in the structure determination: (*a*) the oxygen Crenels giving rise to the octahedral and trigonal prismatic sites; (*b*) the separation between the octahedral (Co1) and trigonal prismatic (Co2) Co atoms.

Table 2. *Final residual factors for $Sr_{14/11}CoO_3$ [commensurate (3+1)-dimensional option]*

	N	R	R_w
Main	519	3.04	3.47
First order	508	3.71	3.21
Second order	126	6.77	5.95
Third order	16	18.22	19.09
Overall	1169	3.51	3.51
CoO_3 part	244	3.76	4.06
Sr part	230	2.57	2.92
Common	45	2.45	3.18

Table 3. *Fractional atomic coordinates and equivalent isotropic displacement parameters ($Å^2$) for $Sr_{14/11}CoO_3$ [commensurate (3 + 1)-dimensional option]*

$$B_{\mathrm{eq}} = \Sigma_i \Sigma_j U^{ij} a_i^* a_j^* a_i a_j.$$

	x	y	z	B_{eq}	τ
Sr	1/3	0	1/4	1.189 (9)	
Co1	0	0	0	0.517 (9)	8/11
Co2	0	0	0	2.17 (3)	3/11
O	0.1546 (2)	0.1546	1/2	1.42 (4)	

Table 4. *Anisotropic displacement parameters U^{ij} ($Å^2$) for $Sr_{14/11}CoO_3$ [commensurate (3 + 1)-dimensional option]*

The anisotropic displacement factor exponent takes the form

$$(-2\pi^2 \Sigma_i \Sigma_j U^{ij} a_i^* a_j^* h_i h_j).$$

	U^{11}	U^{22}	U^{33}	U^{12}	U^{13}	U^{23}
Sr	0.0148 (2)	0.0148	0.0156 (2)	0.00738 (8)	0	0
Co1	0.00645 (12)	0.00645	0.0067 (3)	0.00322 (6)	0	0
Co2	0.0306 (4)	0.0306	0.0214 (10)	0.0153 (2)	0	0
O	0.00645 (12)	0.00645	0.0067 (3)	0.00322 (6)	0	0

wave orders for Co1 (to second order for position and zero for DWF) and suppressing them for Co2, the residual factor dramatically dropped to R = 0.0454 for the same number of parameters (35). The refinement smoothly converged to a residual factor R = 0.0378 for 46 parameters through the increase of the modulation wave order for the description of each atom position and DWF (Co1: 3 + 0; Co2: 1 + 0; O: 3 + 1; Sr: 4 + 4), and the introduction of an isotropic extinction correction (Becker & Coppens, 1974).

In the description of $Sr_{1.2872}NiO_3$ (Evain *et al.*, 1998), a further splitting of the metal in the trigonal prisms was necessary because of the distribution of Ni atoms over three positions in the trigonal prism faces and two positions on the $\bar{3}$ axis. No significant residues could be observed on the difference Fourier maps in the trigonal prism faces (around Co2) for the present description of $Sr_{14/11}CoO_3$. However, at that stage of the refinement the Co2 density was not properly described, as shown in Fig. 3(*a*). To better model this density distribution a splitting of the Co2 position was first attempted. It did

Table 5. *Non-harmonic displacement parameters C_{GC}^{ijk} of Co2 for $Sr_{14/11}CoO_3$ [commensurate (3 + 1)-dimensional option]*

Tensor elements C_{GC}^{ijk} are multiplied by 10^3.

	C_{GC}^{111}	C_{GC}^{112}	C_{GC}^{113}	C_{GC}^{122}	C_{GC}^{123}	C_{GC}^{133}	C_{GC}^{222}	C_{GC}^{223}	C_{GC}^{233}	C_{GC}^{333}
Co2	0	0.0058(4)	0	0.0058	0	0	0	0	0	0

not succeed owing to highly correlated parameters. A third order Gram–Charlier development of the Co2 atomic displacement factor was then tried. With only one extra parameter, the residual factor significantly dropped from 3.78 to 3.54% and the strong residues vanished (see Fig. 3*b*). A test of the overall stoichiometry revealed neither a cobalt nor an oxygen deficiency.

2.4.2. *(3 + 1)-dimensional commensurate option*. The (3 + 1)-dimensional superspace group gives rise to three possible three-dimensional space groups ($P\bar{3}$, $P32$ and $P3$), as a function of the *t*-phase section, for $\gamma = m/n$ with both *m* and *n* odd (Evain *et al.*, 1998). Each possible particular section was tested with the model obtained from the incommensurate option, that is, without new additional parameters. Clearly, the $P\bar{3}$ centrosymmetric space group [$t = 0$ or $t = \pm 1/6n \bmod(1/2n)$] gives much higher residual factors ($R = 0.05$) than the incommensurate option and must be discarded. The $P32$ and $P3$ three-dimensional space-group tests give similar results ($R = 0.0351$ and $R = 0.0352$, respectively), comparable to those obtained with the incommensurate option. Since the **q** vector can be considered as commensurate within 1 e.s.d. and since the results obtained with the incom-

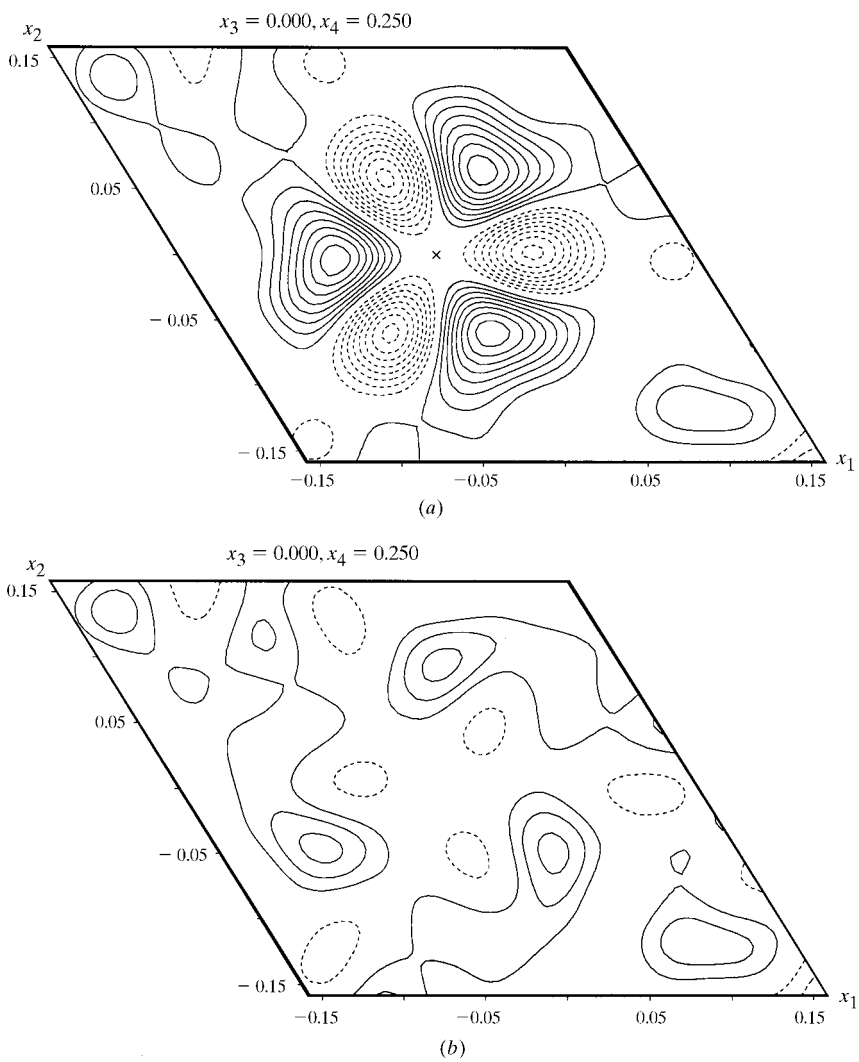

Fig. 3. x_1x_2 section at $x_3 = 0$ and $x_4 = \frac{1}{4}$ of the difference Fourier contour maps around Co2: (*a*) before introducing third-order atomic displacement parameters; (*b*) after introducing one third-order atomic displacement parameter. Contour lines in intervals of 0.2 e Å^{-3} (negative as dashed lines and positive as continuous lines).

mensurate and commensurate models cannot be discriminated, the commensurate model ($P32$ space group) will be the only one discussed thereafter. The final residual factors are $R = 0.0351$ and $wR = 0.0351$ for 47 parameters and 1169 reflections, with a twinning fraction of *ca* 11%. Final results are gathered in Tables 2–5, as obtained from the refinement and in a conventional three-dimensional format (atomic positions only). It is worth noting that a traditional three-dimensional refinement requires 42, 42 and 80 independent atoms and 282, 291 and 558 parameters for the $P32$, $P\bar{3}$ and $P3$ space groups, respectively. Obviously, from the (3 + 1)-dimensional solution, the same R factors are obtained as in the three-dimensional method. However, such an approach leads to highly correlated parameters and quickly diverges.

3. Discussion

$Sr_{14/11}CoO_3$ is a new member in the hexagonal perovskite oxide family of the general formula A_xMO_3. As for $Sr_{1.2872}NiO_3$, the $Sr_{14/11}CoO_3$ structure can be described as an intergrowth of [Sr] and [CoO_3] chains (see Fig. 4). The latter chains are built through face sharing from two different [CoO_6] entities, *i.e.* octahedra (Oh) and trigonal prisms (TP). Within a [CoO_3] chain, the succession of the two entities is $(1TP–3Oh–1TP–2Oh–1TP–3Oh)_\infty$. As previously established (Evain *et al.*, 1998), the Oh/TP ratio can simply be expressed as a function of the γ component of the **q** wavevector: $Oh/TP = 2(1-\gamma)/(2\gamma-1)$, that is Oh/TP = 8/3 in the present case since $\gamma = 7/11$. The TP density is therefore higher than in $Sr_{6/5}CoO_3$, for which Oh/TP = 4/1, and the Oh blocks are shorter than in the latter compound. Assuming an occupation of the octahedra by Co^{IV} and of the trigonal prisms by Co^{II} (see the distance discussion thereafter), the overall charge balance is achieved with $Sr^{II}_{14/11}Co^{IV}_{8/11}Co^{II}_{3/11}O^{II}_3$. A similar charge balance is obtained for $Sr_{6/5}CoO_3$ with $Sr^{II}_{6/5}Co^{IV}_{4/5}Co^{II}_{1/5}O^{-II}_3$. A different formulation with two different neutral fragments, $[Sr^{II}_2Co^{II}O^{-II}_3]_{3/11}[Sr^{II}Co^{IV}O^{-II}_3]_{8/11}$, has also been proposed (Evain *et al.*, 1998). This latter formula explains why several Sr_xCoO_3 phases can be obtained, of which $Sr_{6/5}CoO_3$, $Sr_{14/11}CoO_3$ and $Sr_{24/19}CoO_3$ (not yet fully resolved because of a severe twinning) are the first characterized compounds in the series.

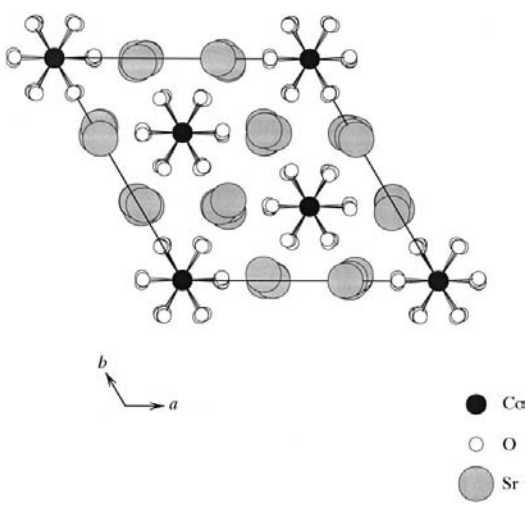

Fig. 4. Projection along the c axis of the $Sr_{14/11}CoO_3$ structure [(3 + 1)-dimensional commensurate model].

Fig. 5(*a*) shows Co—O distances of the [CoO_3] chains plotted as a function of the internal coordinate t, the distances corresponding to the commensurate case being singled out [by crosses for Co at (0,0,z) and by squares for Co at ($\frac{1}{3},\frac{2}{3},z$) or ($\frac{2}{3},\frac{1}{3},z$)]. The Co—O distances observed for the trigonal prisms (Crenels centered at t = 0.25 and t = 0.75) are significantly longer (d_{av}[Co—O] = 2.05 Å) than those found for the octahedra (d_{av}[Co—O] = 1.90 Å). These distances are in very good agreement with those found for a Co^{II} cation in trigonal prismatic sites (2.035 Å in the $[Co_3(OCH_2CH_2NH_2)_6]^{2+}$ trinuclear cation; Bertrand *et al.*, 1969) and for the Co^{IV} cation in octahedral sites (1.874 Å in $BaCoO_3$; Taguchi *et al.*, 1977). They also agree very well with those calculated in $Sr_{6/5}CoO_3$ (1.97 Å for TP and 1.89 Å for Oh; Harrison *et al.*, 1995) and in $Ca_{3/2}CoO_3$ (2.06 Å for TP and 1.92 Å for Oh; Fjellvag *et al.*, 1996).

An important characteristic of this one-dimensional structure is the Co—Co distances along the [CoO_3] chains. These distances are presented in Fig. 5(*b*), where two groups can be distinguished. The shortest distances (d_{av}[Co—Co] = 2.44 Å) correspond to the metal–metal distance between the Oh sites, with a slightly shorter distance between two consecutive Oh sites. The longer distances (d_{av}[Co—Co] = 2.61 Å) are found between the Oh and TP sites. Once again, these distances reasonably match the equivalent distances found in $Sr_{6/5}CoO_3$ (2.44 Å for Oh–Oh and 2.50 Å for Oh–TP) and in $Ca_{3/2}CoO_3$ (2.59 Å for Oh–TP).

Another interesting feature is the non-Gaussian character of the probability density function for the trigonal prism Co atoms (Co2), as depicted in Fig. 6. Although leading to a single mode at the prism center, the deformation towards the prism rectangular faces probably indicates an instability of Co^{II} in the prism center. The observed probability function presumably derives from a static disorder and not from anharmonic vibrations (an assumption that needs, however, to be confirmed through temperature-dependent studies). This is in concordance with the high U_{iso} for the TP Co atom (twice as large as U_{iso} for Oh Co atoms) observed in $Sr_{6/5}CoO_3$ by a neutron powder diffraction experiment. However, this is different from that observed for Ni in $Sr_{1.2872}NiO_3$, where the Ni atoms were found either on the trigonal prism square-like faces or on the three-fold axis, slightly away from the prism center. As in $Sr_{1.2872}NiO_3$, and in contrast with that found in

$Sr_{6/5}CoO_3$, the $[CoO_6]$ prism is not twisted, but almost regular.

The strontium environment is complicated with the shortest Sr—O distance (2.3 Å) being established with the edge of the trigonal prism, a situation already found in $Sr_{6/5}CoO_3$. The Sr atoms are at the cobalt z elevation for the prismatic sites, but at the sulfur level for the octahedra (see Fig. 7). This is observed in all hexagonal perovskite oxides. Contrary to what could be imagined from Fig. 4, the longest Sr—Sr distances are found along the z axis with d_{max}[Sr—Sr] = 4.02 Å and the shortest ones in-between the [Sr] chains with d_{min}[Sr—Sr] = 3.48 Å. Therefore, the Sr—Sr contacts along the chains are not an issue in the change of the Oh/TP alternation between all possible Sr_xCoO_3 phases.

4. Conclusions

A new phase, $Sr_{14/11}CoO_3$, in the hexagonal perovskite Sr_xCoO_3 system has been found and its structure solved from single-crystal X-ray data within the (3 + 1)-dimensional formalism. The structure is similar to that of $Sr_{6/5}CoO_3$, but with a different sequence of the Oh/TP polyhedra along the $[CoO_3]$ chains. An interesting feature of the Sr_xCoO_3 phases, that was not detected in the neutron powder structure determination of $Sr_{6/5}CoO_3$, but which is probably common to all cobalt

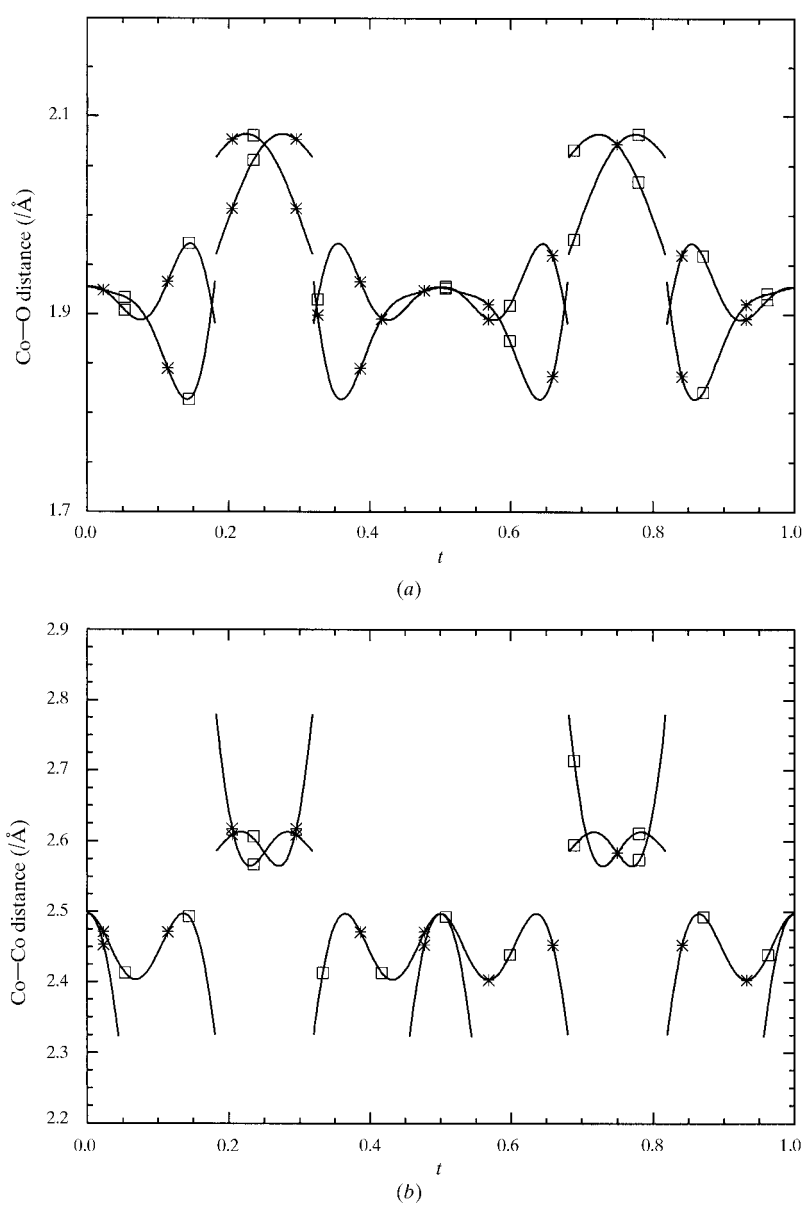

Fig. 5. (*a*) Co—O and (*b*) Co—Co distances (Å) as a function of the internal t coordinate for the (3 + 1)-dimensional commensurate model. Cross and square marks correspond to equivalent distances calculated from the three-dimensional commensurate model (see text).

A_xMO_3 phases, is the displacement of the prismatic Co atoms from the site center, towards the prism rectangular faces. Band structure calculations are currently in progress to explain such a feature. Since several phases with very close compositions can be easily obtained in the Sr_xCoO_3 system (*i.e.* $Sr_{6/5}CoO_3 = Sr_{1.2}CoO_3$, $Sr_{14/11}CoO_3 \simeq Sr_{1.273}CoO_3$ and $Sr_{24/19}CoO_3 \simeq Sr_{1.263}CoO_3$) as in other A_xMO_3 series (Sr_xNiO_3 for instance), special care should be taken when studying the usually very interesting magnetic properties of the hexagonal perovskite compounds. Magnetic property studies should be performed on well characterized single crystals rather than on powders to avoid mixtures of close composition phases.

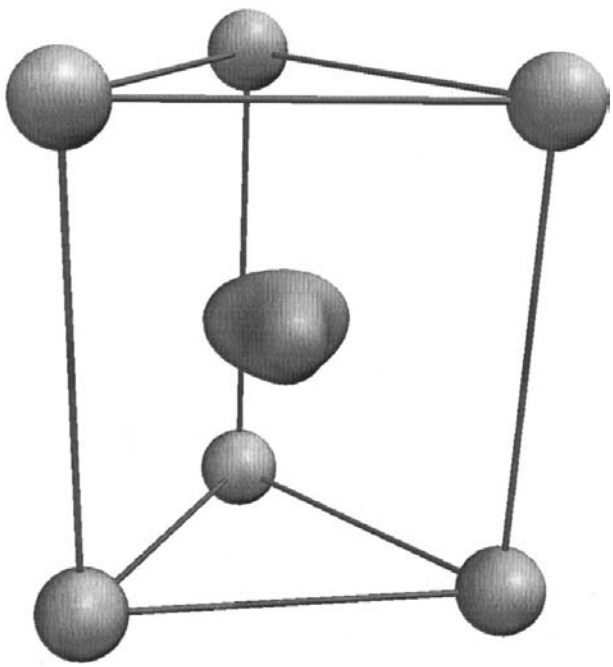

Fig. 6. Three-dimensional representations of cobalt probability density surfaces for the Co2 trigonal prismatic site, indicating a smearing of the density towards the rectangular faces; surface at 5% of the probability density maximum and O atoms represented as spheres of arbitrary size.

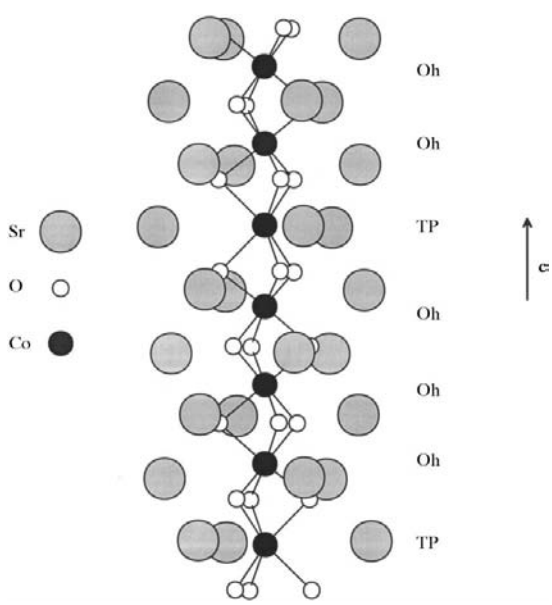

Fig. 7. Projection perpendicular to the *c* axis of one of the $[CoO_3]$ chains and the neighboring Sr atoms for the $Sr_{14/11}CoO_3$ structure [(3 + 1)-dimensional commensurate model].

References

Battle, P. D., Gibb, T. C. & Steel, A. T. (1988). *J. Chem. Soc. Dalton Trans.* pp. 83–87.

Becker, P. J. & Coppens, P. (1974). *Acta Cryst.* A**30**, 129–147.

Bertrand, J. A., Kelley, J. A. & Vassian, E. G. (1969). *J. Am. Chem. Soc.* **91**, 2394–2395.

Bezdicka, P. (1993). Thesis. Université Bordeaux I, France.

Bezdicka, P., Wattiaux, A., Grenier, J.-C., Pouchard, M. & Hagenmuller, P. (1993). *Z. Anorg. Allg. Chem.* **619**, 7–12.

Darriet, J. & Subramanian, M. A. (1995). *J. Mater. Chem.* **5**, 543–552.

Dussarat, C., Grasset, F. & Darriet, J. (1995). *Eur. J. Solid State Inorg. Chem.* **32**, 557–576.

Evain, M. (1992). *U-fit. A Cell Parameter Refinement Program*. Institut des Matériaux Jean Rouxel, Nantes, France.

Evain, M., Boucher, F., Gourdon, O., Petricek, P., Dusek, M. & Bezdicka, P. (1998). *Chem. Mater.* **10**, 3068–3076.

Fjellvag, H., Gulbrandsen, E., Aasland, S., Olsen, A. & Hauback, B. C. (1996). *J. Solid State Chem.* **124**, 190–194.

Harrison, W. T. A., Hegwood, S. L. & Jacobson, A. J. (1995). *J. Chem. Soc. Chem. Commun.* pp. 1953–1954.

Janssen, T., Janner, A., Looijenga-Vos, A. & de Wolff, P. M. (1993). *International Tables for X-ray Crystallography*, Vol. C, ch. 9.8, edited by A. J. C. Wilson. Dordrecht: Kluwer Academic Publishers.

Onoda, M., Saeki, M., Yamamoto, A. & Kato, K. (1993). *Acta Cryst.* B**49**, 929–936.

Petricek, V. & Dusek, M (1998). *JANA98. Programs for Modulated and Composite Crystals.* Institute of Physics, Praha, Czech Republic.

Petricek, V., van de Lee, A. & Evain, M. (1995). *Acta Cryst.* A**51**, 529–535.

Rodriguez, J., Gonzalez-Calbert, M., Grenier, J.-C., Pannetier, J. & Anne, M. (1986). *Solid State Commun.* **62**, 231–234.

Smaalen, S. van (1995). *Crystallogr. Rev.* **4**, 79–202.

Taguchi, H., Takeda, Y., Kanamaru, F., Shimada, M. & Koizumi, M. (1977). *Acta Cryst.* B**33**, 1298–1299.

Takeda, Y., Kanno, R., Takada, T., Yamamoto, O., Takano, M. & Bando, Y. (1986*a*). *Z. Anorg. Allg. Chem.* pp. 259–270.

Takeda, Y., Kanno, R., Takada, T., Yamamoto, O., Takano, M. & Bando, Y. (1986*b*). *Z. Anorg. Allg. Chem.* pp. 540–541.

Trueblood, K. N., Burgi, H.-B., Burzlaff, H., Dunitz, J. D., Gramaccioli, C. M., Schulz, H. H., Shmueli, U. & Abrahams, S. C. (1996). *Acta Cryst.* A**52**, 770–781.

Ukei, K., Yamamoto, A., Watanabe, Y., Shishido, T. & Fukuda, T. (1993). *Acta Cryst.* B**49**, 67–72.

Yamamoto, A. (1982). *Acta Cryst.* A**38**, 87–92.